RESEARCH

Consideration of climate change impacts on a hydropower scheme in Iran

Mohammad Reza Khazaei[1] · Meisam Heidari[2] · Shamsuddin Shahid[3] · Mehraveh Hasirchian[4]

Abstract

Climate change is likely to significantly affect hydropower generation in the future. It is important to assess the impacts of climate change on hydropower plants for their optimal and cost-effective design. This article proposes a modeling framework for assessing climate change impacts on a potential hydropower plant in Iran. A modified version of the LARS-WG model (M-LARS-WG) was used for downscaling the simulations of two global climate models, CanESM2 and HadGEM2, for three emission scenarios RCP2.6, RCP4.5, and RCP8.5, and generating 50 sets of daily weather variables, each covering a 30-year period for the historical period and each future scenario. The generated data was introduced into a calibrated HBV hydrological model to simulate the daily streamflow series of the basin. Finally, the Modified Standard Operating Policy (MSOP) model was employed to simulate reservoir water level and power plant productions under climate change scenarios. The rank-sum test showed the similarity in the average of M-LARS-WG simulated and observed variables in each month at 5% significance. The HBV model estimated the observed streamflow with a Nash–Sutcliffe coefficient of 0.83 during validation. The output of the modeling framework revealed the changes in annual streamflow ranging from a decrease of 35% to an increase of 90% during 2035–2064 compared to the historical period for different climate change scenarios. This would change the hydropower generation between -25 and $+2\%$ compared to the historical period. The study indicates the importance of considering climate change impacts on hydropower plant design.

1 Introduction

Climate change, caused by the combustion of fossil fuels as an energy source, has created significant risks to multiple sectors and made the earth's future uncertain. Countries should reduce their dependence on fossil fuels for energy production and opt for cleaner energy sources (Casale et al. 2020; Mukheibir 2013). Hydropower is an important clean and renewable energy source, and its promotion can

significantly contribute to climate change mitigation. It accounts for more than 16% of total electricity generation and about 85% of renewable electricity generation worldwide (Zhou et al. 2018). However, climate change will impact hydropower generation by changing atmospheric and hydrological processes. Therefore, ignoring the future effects of climate change on hydropower generation could lead to suboptimal performance and economic inefficiency in hydropower generation projects (Carvajal et al. 2017; Lumbroso et al. 2015; Mukheibir 2013; Natalia et al. 2020).

The primary impacts of climate change would be the changes in temperature, precipitation, evapotranspiration, soil moisture, and river flow regime, all of which will affect water resources (Khazaei 2021; Natalia et al. 2020). The energy production in hydropower plants depends on available water resources. Therefore, climate change could significantly affect hydropower generation in the future (Carvajal et al. 2017; IPCC 2007; Mukheibir 2013; Natalia et al. 2020).

Several studies have assessed climate change effects on hydropower generation. IPCC (2007) and Bates et al. (2008) reviewed the available studies and found that climate change

✉ Mohammad Reza Khazaei
m_r_khazaee@yahoo.com; khazaei@pnu.ac.ir

1 Department of Civil Engineering, Payame Noor University, Tehran, Iran

2 Department of Earth and Atmospheric Sciences, Université du Québec À Montréal (UQAM), Montreal, Canada

3 Department of Water & Environmental Engineering, School of Civil Engineering, Faculty of Engineering, Universiti Teknologi Malaysia (UTM), Johor Bahru, 81310 Johor, Malaysia

4 School of Civil Engineering, Iran University of Science and Technology, Tehran, Iran

impacts on hydropower generation in the future would vary significantly across the globe. For example, general predictions for climate change and streamflow in Africa indicate that hydropower resource potential will decrease in Africa (excluding East Africa). It would also decrease by 20–50% in the Mediterranean region of Europe but increase by 15–30% in northern and Eastern Europe by 2070 (Kumar et al. 2011). Carvajal et al. (2017) assessed the impact of climate change on Ecuadorian hydropower plants using projections of 40 GCMs for RCP4.5. They showed that annual hydroelectric power production in Ecuador in 2071–2100 would change between +39 and −55% compared to 1971–2000. Zhou et al. (2018) used a global hydrological model to predict the maximum achievable hydropower generation (MAHG) under two climate change scenarios at the end of this century. They found that the changes in MAHG would vary from −71% in the Middle East to +14% in the Former Soviet Union for RCP8.5. Shrestha et al. (2021) assessed the impact of climate change on the Kulekhani Hydropower Project in Nepal using projections of three Regional Climate Models (RCMs) under the RCP 8.5 scenario up to 2099. They found that precipitation exhibits erratic patterns with dry season increases and wet season decreases, leading to projected hydropower generation reductions by 0.5 to 13% in the future compared to 1983–2009. Zhao et al. (2023) investigate the impact of streamflow drought on hydropower generation in China under climate change. Utilizing global hydrological models and climate models, they project that more than 25% of hydropower plants could face hydropower generation reductions exceeding 20% of baseline hydropower generation. Almeida et al. (2021) assessed the impacts of climate change on hydropower development in the Amazon. They found that under mid-century climate change projections for the RCP4.5 and RCP8.5 scenarios, the Amazon basin could experience reductions in river discharge (13% and 16%, respectively) and hydropower generation (19% and 27%), posing challenges to over 350 proposed dams across the Amazon basin.

As local studies, Stucchi et al. (2019) assessed the climate change impacts on hydropower generation at a plant in Italy using projections of three GCMs under three RCP scenarios. They found that power generation, driven by seasonal demand and water availability, would decrease by 8 to 27% between 2045 and 2059. Zhao et al. (2022) assessed the impact of climate change on hydropower in the Yalong River basin in China. They used the bias correction and spatial disaggregation method to perform statistical downscaling on the 10 Coupled Model Intercomparison Project Phase 6 (CMIP6) models. Then, the downscaled climate scenarios were used to drive a large-scale hydrological model, which was coupled with a reservoir operation module. They estimated the power generation of the basin would be reduced by 4 to 6% in the future compared to the baseline period.

Stucchi et al. (2023) assessed the impacts of climate change on the dynamics of Santa Giustina Lake in Italy, which was exploited by a power plant with a production of 282 GWh/year. They found that due to climate change, the seasonality of streamflow will change so that the streamflow will decrease in spring and summer and increase in winter. Liang et al. (2023) investigated the impact of climate change on the Yalong River Basin. They estimated the future runoff and hydropower generation using the WaterGAP hydrological model based on projections of four GCMs under two RCP scenarios. They found that future hydropower generation would change between −0.87 and 6.10% by 2099 compared to the historical period (1981–2000).

Iran is one of Asia's highest hydropower-producing countries (Kumar et al. 2011). For example, in 2017, a total of 15,300 GWh of hydropower were generated, which was used to assist the system during peak times (Solaymani 2021). However, climate change may significantly affect its potential for generating hydropower (Kumar et al. 2011; Zhou et al. 2018).

It is crucial to assess the effects of future climate change on energy production and consider them in hydropower plant design to prevent suboptimal performance and economic inefficiency (Kumar et al. 2011; Lumbroso et al. 2015; Mukheibir 2013). Particularly, it is essential to consider the effects of climate change on the design of hydroelectric dams due to their long (~100 years) lifespan (Lumbroso et al. 2015).

Climate change effects are often overlooked in hydropower project planning, and hydropower plants are generally designed using historical climate data and based on the assumption of stationarity (Lumbroso et al. 2015; Mukheibir 2013). However, considering climate change, hydropower generation may change in the future, and the stationarity assumption will not be valid (Khazaei 2021; Lumbroso et al. 2015; Milly et al. 2008; Mukheibir 2013).

For accurate quantitative predictions of regional climate change impacts on hydropower generation, it is necessary to simulate the future streamflows. The simulation can be done using a hydrological model fed by GCM simulations at the outlet of a basin (Kumar et al. 2011; Natalia et al. 2020). Given that the resolution of GCM simulations is often too coarse for watershed-scale climate change impact assessment, the development of downscaling methods becomes necessary. Various downscaling methods, including dynamic methods based on regional climate models (RCMs) and statistical methods, have been developed. However, RCMs are not available for many areas (ul Shafiq et al. 2019), where statistical downscaling is commonly used.

For a reliable assessment of climate change impacts on hydrological processes, the downscaling method should preserve the natural cross-correlation between weather variables (at least precipitation and temperature). Among

statistical downscaling methods, the change factor (CF) and weather generator (WG) methods offer this advantage (Khazaei et al. 2020b). The CF is a simple method in which the differences between monthly means of control and future GCM simulations are applied to every baseline observed data series, either as multiplication or summation. It only adjusts the mean climate and ignores changes in variability and other statistics (Fowler et al. 2007; Khazaei et al. 2012). In contrast, WGs can transfer changes in various climatic characteristics, including means, variances, and other important statistics projected by GCMs, to the downscaled climate series (Fowler et al. 2007; Khazaei 2021). Moreover, WGs can generate arbitrarily long synthetic time series of climate variables, representing a wide range of possible situations. This reduces the uncertainty of climate variability and improves the accuracy of impact analyses (Khazaei et al. 2020a, 2020b; Semenov et al. 1998).

Khazaei et al. (2020b) proposed a new method for improving the performance of the Long Ashton Research Station-Weather Generator (LARS-WG) model and developed the Modified LARS-WG (M-LARS-WG) model. The modifications improved the WG performance in reproducing low-frequency (inter-annual) variability (LFV) and downscaling performance. Moreover, it improved the performance of the WG in reproducing a wide range of other observed weather characteristics. It is essential to correctly model variabilities because increasing climate variability can reduce hydropower potential even without changing the streamflow average (Kumar et al. 2011). It is also imperative to model inter-annual variability to encompass extreme events properly.

This paper proposes a robust method for assessing future climate change impacts on a hydropower plant scheme in Iran. The M-LARS-WG model (Khazaei et al. 2020b) was used for downscaling and generating long-term daily weather series. The HBV (Hydrologiska Byråns Vattenbalansavdelning) hydrological model was used to simulate daily basin flow from climate variables. Finally, the generated long-term daily weather data was used in the framework to assess the effects of climate change on basin flow, reservoir storage characteristics, and hydropower generation. Simulations of two GCMs for three emission scenarios were used to assess the uncertainties in projections. Additionally, 50 synthetic series of each variable for 30 years were generated for the historical period and future scenarios to reduce uncertainty due to natural climate variability in projections. The framework proposed in this study, comprising climate downscaling, hydrological simulation, and reservoir models, can be used for a reliable assessment of climate change impacts on hydropower potential in any other region.

Table 1 The reservoir and hydropower plant specifications

H_{min} (m)	H_{max} (m)	S_{max} (MCM)	S_{min} (MCM)	Installed capacity of the power plant (MW)
95	140	544	130	124

H_{min} and S_{min} are the minimum water level and the minimum storage of the reservoir, respectively, and H_{max} and S_{max} is normal water level and storage capacity of the reservoir, respectively

Table 2 GCMs used in this study

GCM	Institute	Resolution (degree)
CanESM2	Canadian Centre for Climate Modelling and Analysis	$2.81° \times 2.81°$
HadGEM2-ES	Met Office Hadley Centre, UK	$1.875° \times 1.25°$

2 Methods and data

2.1 Case study

The studied hydropower plant is a potential power plant dam for construction at the outlet of the Bashar river basin. The Bashar River is a tributary of the Karun River in southwestern Iran, situated in the geographical range of 30°N and 31°N and 51° E to 52° E. The Bashar basin covers an area of 2800 km^2, the average altitude is 2277 m (a.m.s.l.), and its average flow is 52.2 m^3/s. Downstream from this potential dam, several large hydroelectric dams are constructed in a cascading formation on the Karun River.

The reservoir and hydropower plant specifications are presented in Table 1. The power plant is designed to generate electricity during peak hours, with operating and efficiency coefficients of 0.25 and 0.85, respectively. The power plant is designed to work at the maximum capacity. The following constraints are considered for the hydropower plant design. The ratio of the total actual hydropower production to the maximum plant power must be greater than 0.95, and the ratio between the total number of days that the power plant works at maximum capacity to the total number of days simulated should be greater than 0.90. Similar constraints were considered for the design of the Khersan3 hydropower plant, which is located downstream of the current hydropower plant (IWPCO 2009).

This study used daily precipitation and temperature data for 30 years recorded at Yasuj meteorological station, located near the centroid of the basin, and daily streamflow data for 8 years measured at the Pataveh station, located at outlet of the basin. Daily precipitation, minimum temperature (T_{min}), and maximum temperature (T_{max}) data of HadGEM2-ES and CanESM2 climate models

(Table 2) were used for climate change impact assessment. HadGEM2-ES and CanESM2 are frequently used to assess climate change impacts in Iran and have shown relatively good performance compared to other GCMs in Iran (Radmanesh et al. 2022; Zamani et al. 2020). In addition, they have relatively different projections over the study basin. The study used models' simulations for the historical period of 1974–2003 and the future periods of 2035–2064 for RCP2.6, RCP4.5, and RCP8.5. The RCPs are described in Table 3 (IPCC A 2013).

2.2 Steps of climate change impact assessment

1. Climate change impact assessment on the hydropower generation and dam reservoir was conducted using the following steps:
2. Daily future precipitation, T_{max}, and T_{min} simulations of the GCMs were downscaled at the Yasuj meteorological station using M-LARS-WG model. This model was then used to produce 50 30-year series of each variable for the historical period and individual future scenarios.
3. The HBV hydrological model was calibrated and validated to simulate the rainfall-runoff process upstream of the dam.
4. The data generated in step 1 were introduced into the HBV model, and the long-term (50 30-year) streamflow series were generated for the historical period and future scenarios.

5. A simulation model was developed for the dam reservoir and the hydroelectric power plant.
6. The streamflow data generated in step 3 and the temperature in step 1 (which were converted to the temperature of the reservoir site by the temperature-altitude relationships) were introduced into the reservoir model to generate the daily data of the reservoir storage, the reservoir water level, the dam spill, and hydropower for historical period and future scenarios.
7. The statistical characteristics of the variables for the historical period and future scenarios were compared to assess the effect of climate change.

The methodology is also presented in Fig. 1.

2.3 M-LARS-WG downscaling model

In the M-LARS-WG model, the daily precipitation, T_{max}, and T_{min} series are first generated by the LARS-WG model. The LARS-WG is a daily stochastic WG that generates synthetic precipitation, T_{max}, T_{min}, and solar radiation series at a location. This model uses semi-empirical probability distributions of weather variables for data generation. The distributions, autocorrelation, and cross-correlation parameters of each variable for each month of the year are estimated from the observed weather data series. For data generation, wet and dry series, the lengths approximated by semi-empirical probability distributions are ordered alternately (one after

Table 3 RCPs used in this study

RCP	Description
RCP2.6	The value of the radiative forcing (RF) peaks at 3 W/m^2 before 2100 and then declines to approximately 2.6 W/m^2 by 2100
RCP4.5	The value of RF is stabilized at 4.5 W/m^2 around 2100, without overshoot
RCP8.5	The value of RF will increase by 8.5 W/m^2 by 2100

Fig. 1 Flowchart of the research method
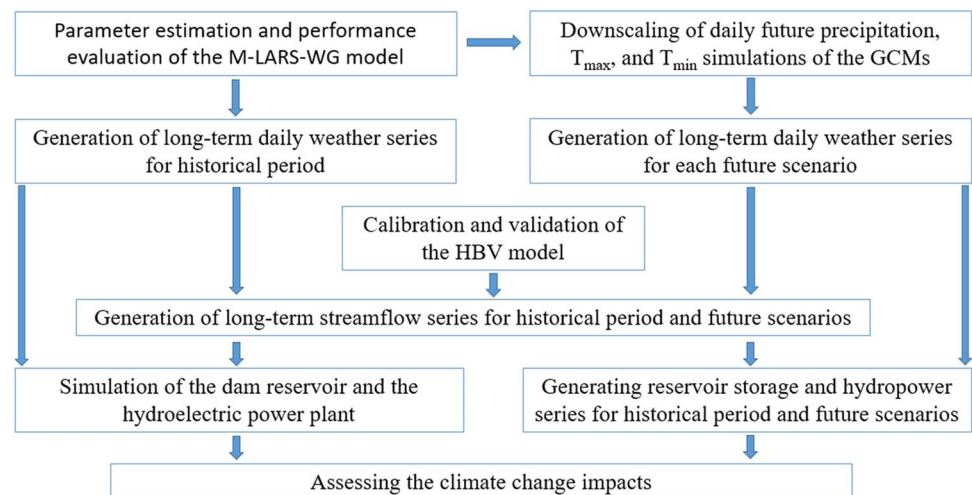
the other). For a wet day, the amount of rainfall is then randomly selected using the semi-empirical distribution for that month. To simulate the T_{max} and T_{min} series, the daily means and standard deviations cycle of the observed T_{max} and T_{min} are reduced separately for dry and wet days. Autocorrelation and cross-correlation between T_{max} and T_{min} are modeled by applying the first-order multivariate autoregressive model (AR (1)) to the normalized residuals. The T_{max} and T_{min} for dry and wet days are approximated by semi-empirical distributions. More information about LARS-WG is provided in Semenov and Stratonovitch (2010).

In the M-LARS-WG, the LFV of the daily synthetic precipitation, T_{max}, and T_{min} series, generated by the LARS-WG, is modified using the following methods. To correct the LFV of the precipitation series, the frequency distribution of monthly precipitation obtained from the output of the LARS-WG model is matched to the frequency distribution of monthly observed precipitation using the quantile perturbation method. To this end, the generated daily precipitation values in each month of the time series are multiplied by a correction factor to match the precipitation produced in that month to the observed precipitation with the same probability from the observed monthly precipitation frequency distribution. Consequently, the generated monthly precipitation statistics are matched with the observed monthly precipitation statistics, and the LFV of precipitation is corrected.

To correct the LFV of the temperature series, the monthly T_{max} and T_{min} series are generated by a 3-variate monthly AR (1) model, which is dependent on the modified monthly precipitation series in the previous step. Then, the LARS-WG generated monthly mean series of T_{max} and T_{min} is matched with those of T_{max} and T_{min} produced by the monthly model.

The parameters of the M-LARS-WG are estimated from the observed weather data in the 1974–2003 period, and the performance of the model to reproduce observed weather characteristics is evaluated for this period.

To generate future downscaled scenarios using M-LARS-WG, the daily model (LARS-WG), monthly model, and monthly precipitation distributions must be adjusted based on future scenarios. Regarding the LARS-WG model and the monthly temperature model, change fields for the future scenario for each statistic compared to the control period of the GCM outputs are applied to the corresponding observed statistics to obtain future perturbed statistics.

The observed monthly precipitation distribution in each month of the year is converted to the future precipitation distribution by the quantile perturbation downscaling method. To this end, the ratio of the change in the amount of future precipitation to the control precipitation is calculated from the GCM outputs in each month of the year and for each probability of non-exceedance. It is then multiplied by the precipitation corresponding to that month and the probability from the empirical CFD of monthly observed precipitation to obtain the downscaled future empirical CFD of monthly precipitation of the station.

The future downscaled scenarios are generated by M-LARS-WG using perturbed statistics instead of the observed statistics. Moreover, downscaled future empirical CFDs of monthly precipitation are used instead of the empirical CFDs of monthly observed precipitation. Further details of the M-LARS-WG model are provided in Khazaei et al. (2020b).

2.4 HBV rainfall-runoff model

The daily streamflow of the basin was simulated using the semi-distributed continuous HBV rainfall-runoff model. The HBV model is developed by the Swedish Meteorological and Hydrological Institute in the 1970s to aid in the operation of power plant reservoirs (Bergström et al. 1992). This model has been widely used for streamflow forecasting and climate change impact assessment in catchments with different climatic conditions in more than 40 countries and has shown high capability in flow simulation (Nonki et al. 2019; Seibert and Vis 2012). A reason for using the HBV model in this study is that it needs a few parameters, a simple integrated structure, little input data, and a user-friendly interface to produce the streamflow of the basin with appropriate accuracy (Abebe et al. 2010).

The HBV-Light version used in this study can perform 20 elevation levels to divide the basin and sub-basins (Bizuneh et al. 2021). HBV-Light has the components of snow accumulation and melting, soil moisture calculation, runoff production, and flow routing (Seibert and Vis 2012). The structure of this model is shown in Fig. 2. The input climatic variables of the model are precipitation, evapotranspiration, and average daily temperature, and its output is the daily flow of the basin (Nonki et al. 2021). Basin potential evapotranspiration was calculated from daily temperature data using the method of Hargreaves and Samani (1985), calibrated for the studied basin by Khazaei et al. (2014). The HBV model has 14 parameters which are determined during model calibration with an automated optimization tool that combines the genetic algorithm and the Powell optimization method (GAP). Figure 2 shows that the values of Q0, Q1, and Q2 correspond to the runoff output simulated from the routing routine in the standard structure of the model.

The HBV rainfall-runoff model was calibrated and validated for the Bashar basin using two separate four-year daily streamflow data at the Pataveh station and daily precipitation and temperature data at Yasuj meteorological station. The model was calibrated using data from the water years of 1995–1996 (October 1995–September 1996), 1996–1997, 1998–1999, and 2001–2002. Then it was validated using data from the water years of 1981–1982, 1983–1984, 1985–1986, and 1994–1995. The streamflow series of the

Fig. 2 Flowchart representing the HBV model (Reproduced from Seibert (2000))
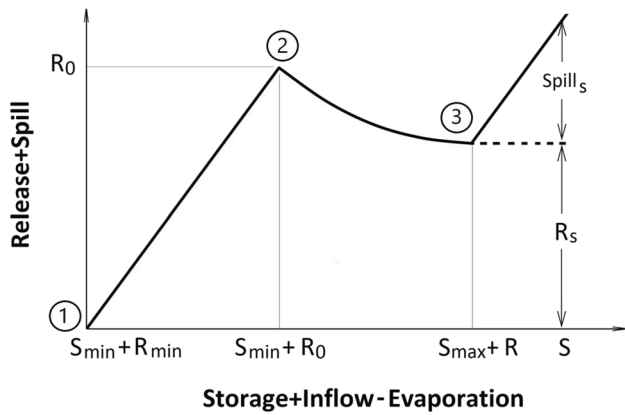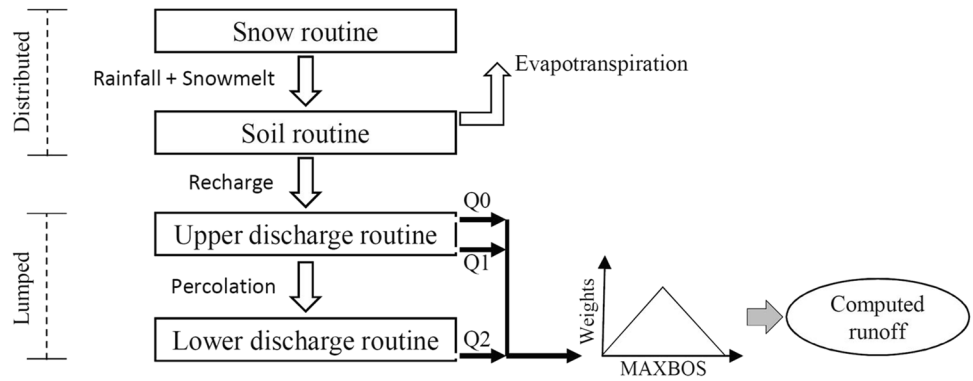

Fig. 3 The scheme of the Modified Standard Operating Policy for hydropower generation

basin was simulated between 1974 and 2003 in each of the calibration and validation stages. However, since only 8 years of reliable observed daily streamflow data were available (Khazaei et al. 2014), the model was calibrated and validated using these 8 years.

2.5 Reservoir operation and hydropower models

The hydroelectric dam reservoir was simulated by the Modified Standard Operating Policy (MSOP) (Tayebiyan et al. 2016), as shown in Fig. 3. Similar to the Standard Operating Policy (SOP), all accessible water is released in MSOP (between points 1 and 2 in Fig. 3) if accessible water is less than the target demand in a time step. On the other hand, the excess water spills (the right side of point 3) if the available water exceeds the total demand and reservoir's storage capacity in a one-time step. Demand is released between points 2 and 3 (Loucks and Van Beek 2017; Tayebiyan et al. 2016). However, in MSOP (different from SOP), the hydroelectric power plant's target demand (D_t) varies based on the nonlinear relationship

between head and demand (Eq. 7). This is because the head increases with increasing storage, and the water demand decreases since the water required to produce a specified target power depends on the head (Neelakantan and Sasireka 2013; Tayebiyan et al. 2016).

The reservoir simulation model is presented by the following equations,

$$S_{t+1} = S_t + I_t - R_t - E_t - Spill_t \quad S_{min} \le S_t \le S_{max} \tag{1}$$

where S_{min} is the minimum storage of the reservoir at the minimum water level, S_{max} is the storage capacity of the reservoir, $S_{(t+1)}$ is the reservoir storage at the end of day t, S_t is the reservoir storage at the beginning of the day t, and I_t is the inflow to the reservoir during day t obtained by simulating the rainfall-runoff process in basin's upstream. R_t is the volume of released water during day t, E_t is the volume of evaporation from the surface of the reservoir lake during day t, and $Spill_t$ is the volume of spill during day t. In Eq. (1), the unit of variables is million cubic meters (MCM).

The spill value is calculated from the following equation,

$$Spill_t = \begin{cases} S_t + I_t - R_t - E_t - S_{max} \\ if S_t + I_t - R_t - E_t > S_{max} \\ \\ 0 \; Otherwise \end{cases} \tag{2}$$

The amount of evaporation from the lake is calculated from the following equation,

$$E_t = 1000 \times K_t \times e_t \times A_t \tag{3}$$

where A_t is the reservoir surface area (km^2) in day t, obtained from the reservoir-storage relationship. K_t is pan coefficient in day t, and e_t is the depth of evaporation (mm) during day t. In the historical period, e_t is calculated from the recorded pan evaporation data. However, since pan evaporation data are not available in the future (to calculate the effects of

climate change), an empirical linear relationship between recorded pan evaporation and temperature data was derived (Eq. 4). Empirical linear relationships between temperature and evaporation were previously used by other researchers (Felfelani et al. 2013).

$$e_t = Max\big[(0.3456 \times T_{\text{mean.t}} - 1.1654) and 0\big] \qquad (4)$$

where $T_{(\text{mean.t})}$ is the average daily temperature (°C) on day t. A_t (km^2) is calculated from Eq. (5) depending on the water level in the reservoir (H_t) (in meters relative to the level of the toe of the dam).

$$A_t = \begin{cases} 0.051 \times H_t - 1.229 & if H_t \leq 90 \\ 0.256 \times H_t - 21.43 & Otherwise \end{cases} \qquad (5)$$

The water level in the reservoir is calculated based on the storage-head relationship obtained from the reservoir topography:

$$H_t = \begin{cases} S_t/(7 \times 10^{-12})^{1/3.676} & if H_t \leq 90 \\ S_t/(7 \times 10^{-10})^{1/3.096} & Otherwise \end{cases} \qquad (6)$$

where S_t is the storage value (MCM) in day t.

The water demand (D_t) in day t (for the hydropower to work at maximum capacity) is calculated based on target power from the following equation,

$$D_t = \frac{P \times 86400}{\xi \times 9806 \times H_{\text{HP.t}}} \qquad (7)$$

where P is the capacity of the power plant in megawatts. $H_{(\text{HP.t})}$ is the difference between the water level of the dam and the power plant runoff in day t, and ξ is the efficiency of the power plant, with an assumed value of 0.85. Release value (R_t) equals the minimum of two available water values and D_t. Next, the energy (MWh) produced in day t is calculated from the following equation,

$$En_t = 2.72 \times R_t \times \xi \times H_{\text{HP.t}} \qquad (8)$$

3 Results and discussion

3.1 Calibration and validation of hydrological models

In the HBV model calibration stage, the Nash–Sutcliffe coefficient (N-S) for daily data was equal to 0.85, and the determination coefficient (R^2) was equal to 0.86. In the validation stage, N-S and R^2 were 0.83 and 0.86, respectively. Compared to other studies, e.g., Zhang and Savenije (2005) and Kamali et al. (2007) and their acceptable criteria (N-S > 0.6 or 0.7), the obtained values are significantly close to the ideal value (i.e., 1), which indicates the proper performance of the hydrological model in simulating the daily flow of the basin. Figure 4 compares the daily streamflows simulated by the HBV model with the corresponding observed streamflows in the calibration and validation stages.

3.2 Performance evaluation of M-LARS-WG

Figure 5 shows the performance of the M-LARS-WG model in simulating precipitation, T_{max}, and T_{min}. In all months of the year, the averages of the simulated data match well with the corresponding observed values. The results indicate that the performance of the M-LARS-WG model is good for simulating the basin meteorological data. Khazaei et al. (2020b) showed that the M-LARS-WG model reproduces a wide range of different observed data characteristics in the simulated data.

Figure 6 presents the results obtained by coupling the M-LARS-WG with the HBV model. Monthly averages (Fig. 6a) and flow duration curves (Fig. 6b) are compared for the streamflows simulated based on the observed weather series and 50 30-year weather series generated by M-LARS-WG. The results show that the simulated flows based on the simulated weather series match the simulated flows based on the observed weather series. This indicates that the simulated basin streamflow is reliable when the outputs of M-LARS-WG are used as inputs to the HBV hydrological model.

Fig. 4 Comparison of the observed and simulated daily streamflow during calibration and validation stages
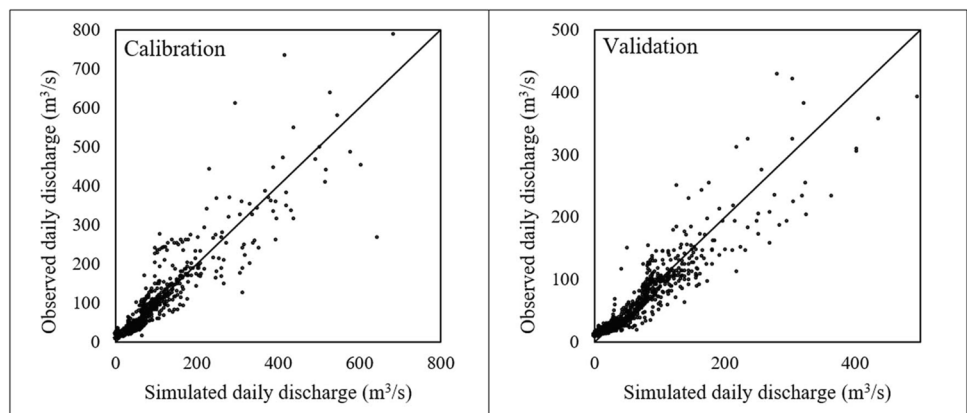
Table 4 presents the *p*-value values of the rank-sum test used to compare the averages of the simulated and observed variables in each month of the year, where

p-value > 0.05 means that the performance of the models is acceptable at a significant level of 5%. The *p*-values for all tests were much larger than 0.05, which indicates
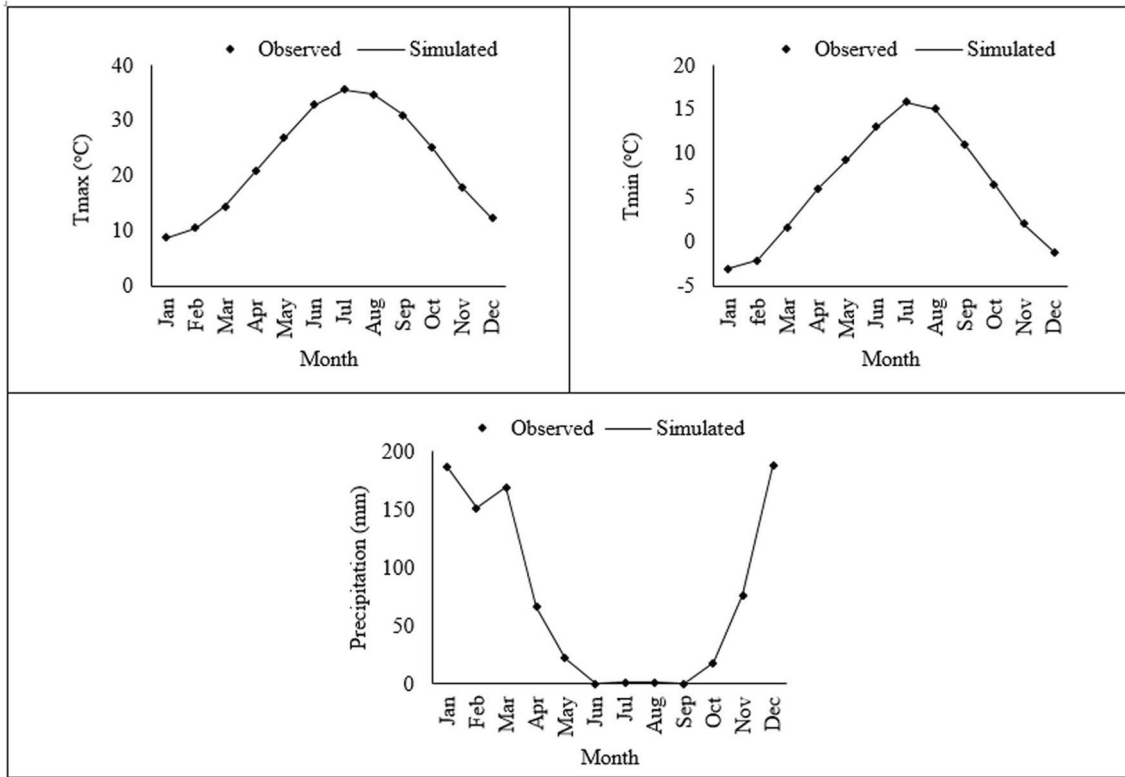

Fig. 5 Performance of M-LARS-WG in reproducing the monthly mean of observed precipitation, T_{max}, and T_{min} series

Fig. 6 Comparison of monthly mean streamflows (**a**) and flow duration curves (**b**) simulated using the HBV model based on the observed weather series and the 50 30-year weather series generated by M-LARS-WG
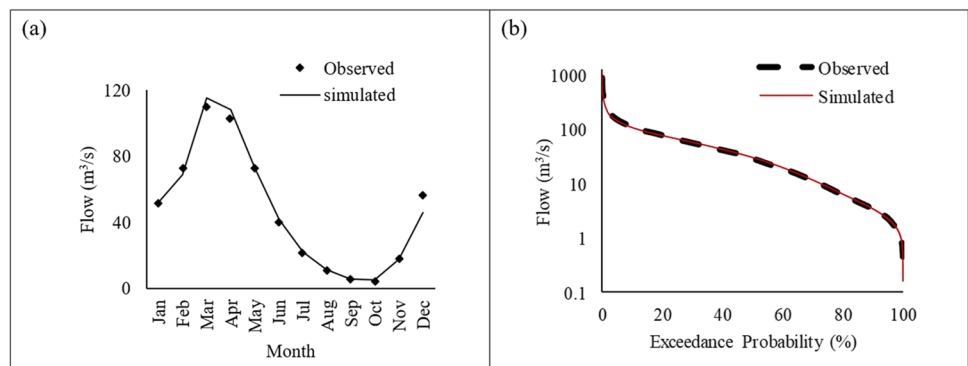
Table 4 The *p*-values of the rank-sum tests used to compare the means of the observed and generated weather variables by M-LARS-WG and the streamflow by the coupled M-LARS-WG and HBV models

	Jan	Feb	Mar	Apr	May	Jun	Jul	Aug	Sep	Oct	Nov	Dec
Precipitation	0.99	0.94	1.00	0.99	0.95	0.67	0.61	0.26	0.99	0.60	0.85	0.97
T_{max}	0.94	0.67	0.91	0.96	0.78	0.75	0.75	0.85	0.86	0.57	0.73	0.67
T_{min}	0.92	0.45	0.65	0.93	0.77	0.61	0.55	0.47	0.38	0.47	0.55	0.98
Streamflow	0.65	0.86	0.23	0.55	0.66	0.45	0.40	0.45	0.41	0.79	0.77	0.85

the good performance of the models. Consequently, the M-LARS-WG model can be used to simulate the meteorological variables of the basin, and the HBV model coupled with M-LARS-WG can be used to simulate the basin streamflow.

3.3 Climate change impacts

Figure 7 shows the climate change impacts for RCP2.6, RCP4.5, and RCP8.5 based on the CanESM2 model. The monthly means of the 1500 years (50 series of 30 years) simulated variables for the historical period are compared with the
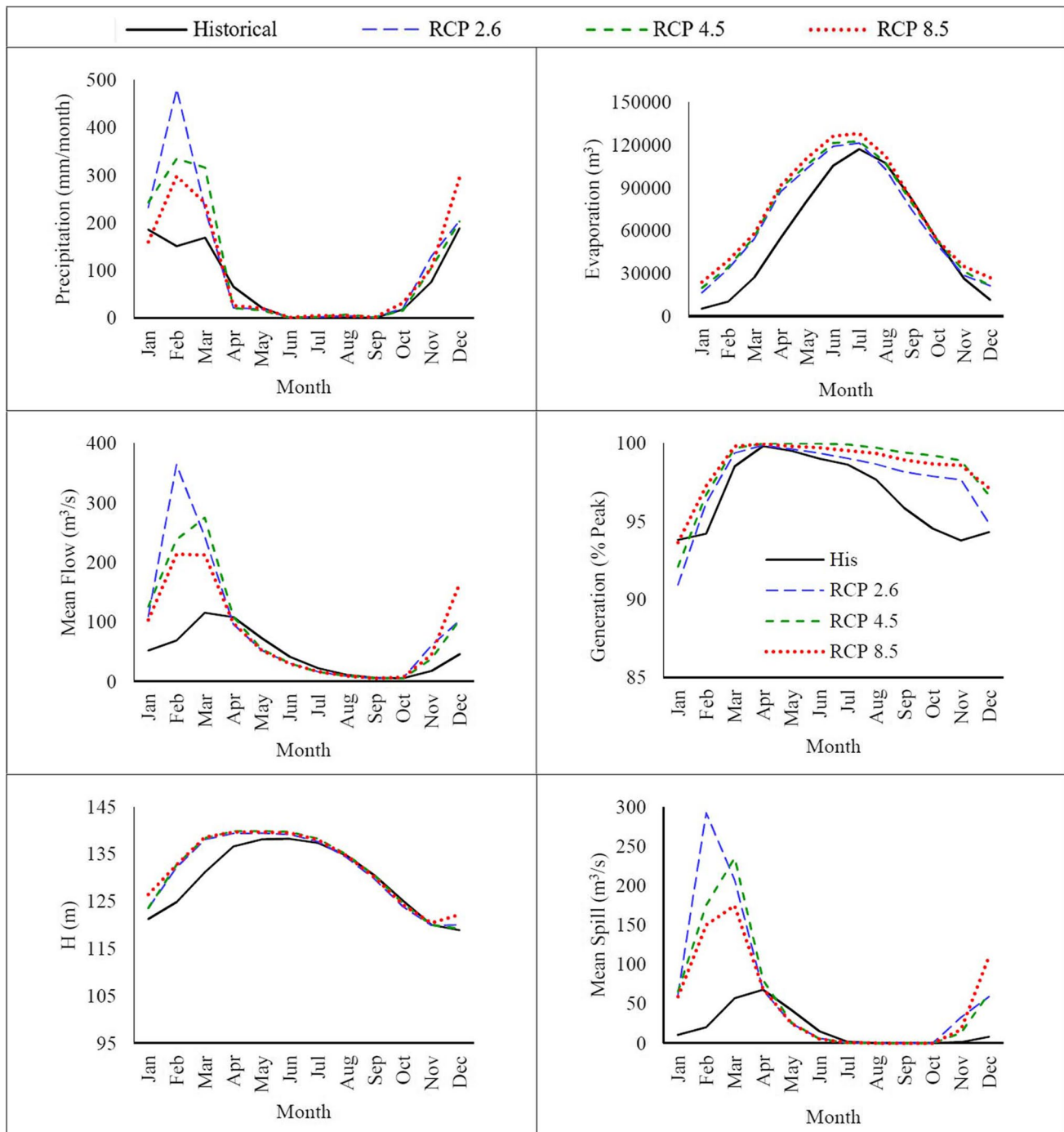

Fig. 7 Climate change impacts on streamflow, hydropower generation, reservoir water levels (H), evaporation from the reservoir, and spill flow, estimated using the CanESM2 model under RCP2.6, RCP4.5, and RCP8.5 for 2035–2064

corresponding values for each future scenario. The results indicate that the average streamflow will increase significantly in the first 3 months (January–March) and the last 2 months of the year (November and December); on the contrary, it will decrease from April to August. The changes in future spill flow are almost similar to that in the reservoir inflow. The reservoir water level will increase significantly in December and in the months from January to July, and evaporation from the reservoir will increase in these months under the influence of changes in temperature and the water surface area of the reservoir. As a result of these changes, the power plant output will increase in all months, except January, under all emission scenarios.

Figure 8 shows the climate change impacts for RCP2.6-, RCP4.5-, and RCP8.5-based HadGEM2 model. The results show that the average streamflow to the reservoir will decrease in almost all months of the year. The average spill discharge will also decrease in the future in all months. Likewise, the reservoir water level will decrease significantly in all months for all scenarios. The evaporation from the reservoir is projected to increase from November to February and decreases from April to September. These evaporation changes depend on changes in the temperature and water surface area of the reservoir. The latter also depends on the water level in the reservoir. As a result of these changes,
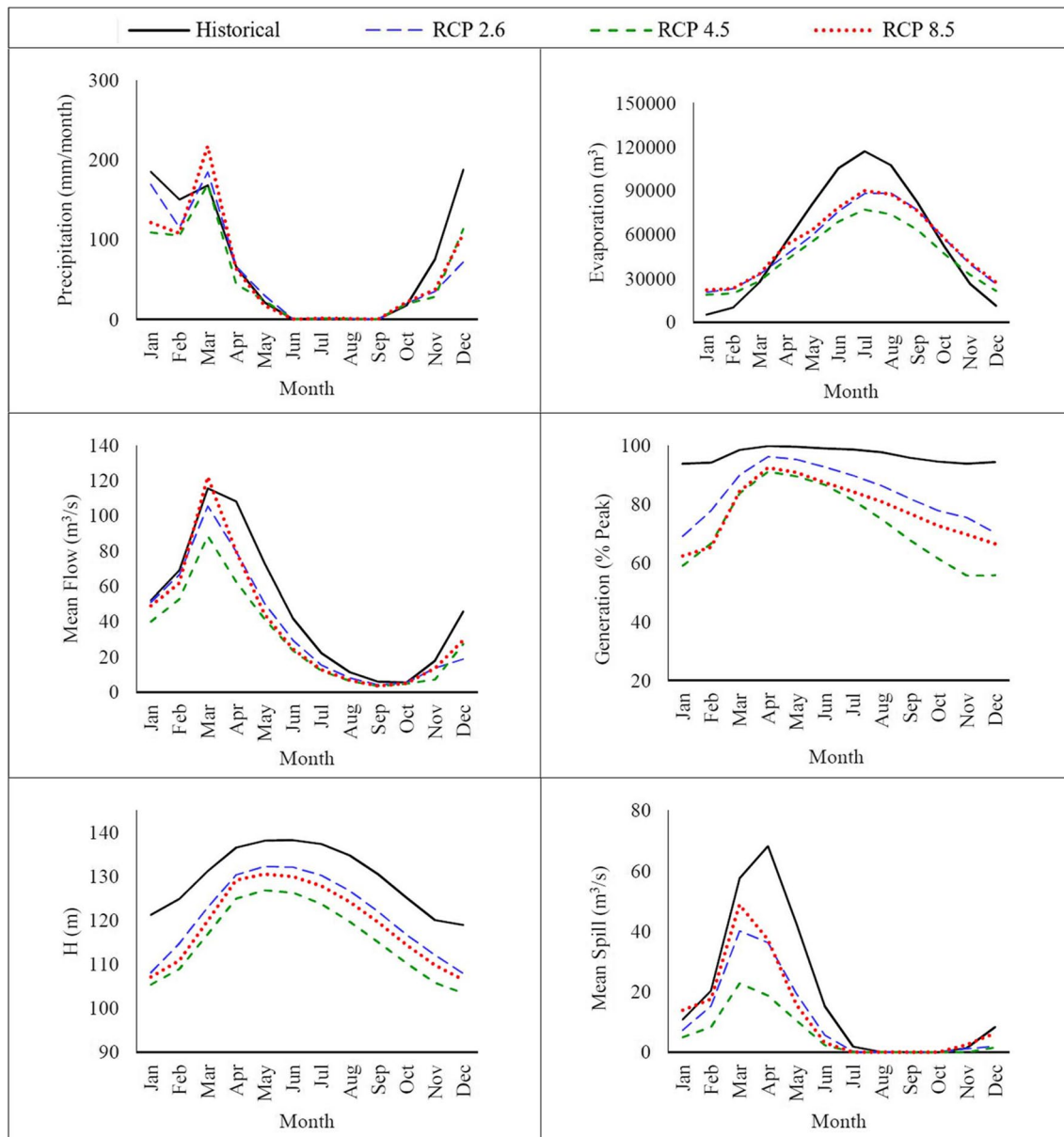

Fig. 8 Climate change impacts on streamflow, hydropower generation, reservoir water levels (H), evaporation from the reservoir, and spill flow, estimated using the HadGEM2 model under RCP2.6, RCP4.5, and RCP8.5 for 2035–2064

the power plant output will decrease in all months of the year under all emission scenarios. The maximum decrease would reach up to 56% of the plant's capacity, particularly in December, under the RCP4.5 scenario.

Monthly statistics of precipitation, T_{min}, T_{max}, streamflow, and hydropower generation over the historical period and future scenarios are presented in Table 1.s to 5.s in the Supplementary Information.

Figure 9 shows the changes in mean temperature, precipitation, streamflow, and power generation for the future period (2035–2064) compared to the historical period (1974–2003), based on the CanESM2 and HadGEM2 projections under RCP2.6, RCP4.5, and RCP8.5 scenarios. The magnitude of change depends on the choice of scenario and GCM. The expected changes in temperature are consistent among GCMs, under the same RCP scenario. For precipitation, streamflow, and electricity generation, the differences between GCMs are considerable. While precipitation, streamflow, and electricity generation will increase based on the CanESM2 projections, they will decrease based on the HadGEM2 projections under all

emission scenarios in the future. Streamflow changes are coherent with precipitation changes. Based on the CanESM2 projections, the mean change in streamflow is slightly larger than precipitation changes, which could be a result of the change in the seasonality of the precipitation. Based on the CanESM2 projections, despite the increase in streamflow will be between 67 and 93%, hydropower generation will increase between 1 and 2%, which is limited according to the capacity of the power plant. Based on the HadGEM2 projections, stream flow will decrease between 20 and 35%, and hydropower generation will decrease between 13 and 25%.

The results show that the uncertainty caused by GCMs and emission scenarios is significant. A large uncertainty in future hydropower generation from GCMs and emission scenarios has been reported by various other studies that have assessed the impact of climate change on hydropower generation (Carvajal et al. 2017; Mousavi et al. 2018; Oyerinde et al. 2016; Qin et al. 2020; Stucchi et al. 2023). These studies generally provide decision-makers with the results of a set of future scenarios for adopting the optimal solution

Fig. 9 Projected changes in temperature, precipitation, streamflow, and power generation for the future period (2035–2064) compared to the historical period (1974–2003)
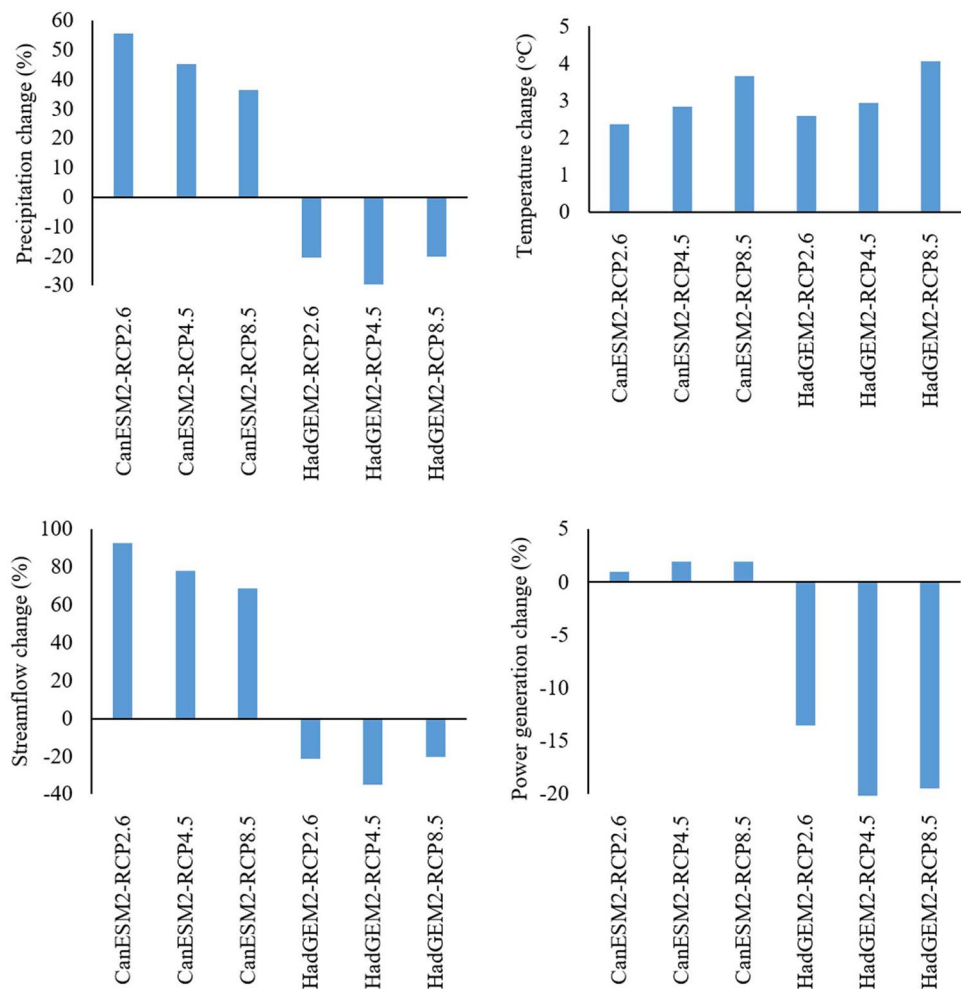
(Carvajal et al. 2017, 2019; Mousavi et al. 2018; Qin et al. 2020) which may be depended on their project conditions.

The current scheme was initially designed to meet the plant design constraints for 50 30-year synthetic hydroclimate series for a historical period (instead of a 30-year observed series) to consider the uncertainty of climate variability and the wide range of feasible situations that may occur during the lifetime of the power plant (without considering climate change). Then, in this paper, the sensitivity of its performance to the climate change impacts was assessed. The results showed that under three of the six future projections, the scheme will significantly fail to meet the plant design constraints (for instance, the total energy generation deficit will exceed 5%). So, it is also necessary to consider the impacts of future climate change in order to prevent the project from failing during the lifetime of the power plant. Several future climate scenarios have been projected by two GCMs under future emission scenarios, while it is not possible to assign probabilities to the climate scenarios (Schaefli 2015). The uncertainty caused by GCMs is significant, and it is not clear which of the future projections will occur. Using more GCMs provides more possible situations that may occur in the future and provides a more reliable design for the power plant. Therefore, it is suggested to consider a wider set of possible future scenarios by using the outputs of a large number of GCMs, and that the set of all these scenarios be used together in the design of the power plant to meet the design constraints for all future scenarios. If the power plant designed based on all future scenarios has a lower capacity than the historical period, it is suggested that the future scenarios serve as the basis for the design.

4 Conclusion

The present study evaluated the potential impact of climate change on the electricity generation of a potential hydropower scheme located in the Bashar River basin of Iran, which was designed based on historical data. The sensitivity of the scheme's performance to the future impacts of climate change was analyzed. Moreover, this paper aims to propose a reliable method for assessing the climate change impacts on hydropower generation.

Future scenarios of T_{min}, T_{max}, and precipitation of the two CanESM2 and HadGEM2 models were downscaled for three scenarios of RCP2.6, RCP4.5, and RCP8.5 using the M-LARS-WG model. As such, the uncertainties of GCMs and emission scenarios were considered here.

Using the M-LARS-WG model, 50 sets of daily climate variables, each covering a 30-year period, were generated for the historical period and each future scenario to provide a wide range of climatic situations and reduce the uncertainty of natural climatic variability. The daily HBV hydrological model was calibrated for the basin with good accuracy. The long-term streamflow of the basin was simulated for historical periods and future scenarios by introducing the M-LARS-WG model outputs to the HBV model. Dam reservoir was simulated by the MSOP method. Hydropower generation of the plant was simulated, and climate change impacts on streamflow, reservoir storage, and hydropower generation were assessed.

The results showed the good performance of the models, including M-LARS-WG, HBV, and their coupling, in simulating the variables. The climate change impact revealed that the average streamflow will decrease under all scenarios in spring and summer during 2035–2064 compared to the historical period. The amount of this reduction is between 15 and 43%. For HadGEM2, the annual streamflow will decrease by 20–35%, while it will increase by 67–93% for CanESM2 due to a significant increase in winter streamflow. HadGEM2 projected a reduction of hydropower generation by 13–25%, while CanESM2 projected an increase of 1–2% during 2035–2064. It is noteworthy that an increase in hydropower generation is limited to the power plant's capacity.

In the present study, future hydropower generation scenarios were produced using a methodological framework comprised of multiple models. The results revealed that climate change could have significant impacts on hydropower generation. As a result, it is essential to use future scenarios instead of historical data to design a hydropower plant and analyze its economic efficiency. In the future, more GCMs and shared socioeconomic pathways (SSPs) can be used in such a study to address uncertainties associated with GCMs.

Declarations

References

Abebe NA, Ogden FL, Pradhan NR (2010) Sensitivity and uncertainty analysis of the conceptual HBV rainfall–runoff model: Implications for parameter estimation. J Hydrol 389:301–310

Almeida RM et al (2021) Climate change may impair electricity generation and economic viability of future Amazon hydropower. Glob Environ Chang 71:102383

Bates BC, Kundzewicz ZW, Wu S, Palutikof JP (2008) Climate Change and Water. Technical Paper of the Intergovernmental Panel on Climate Change, IPCC Secretariat, Geneva, pp 210

Bergström S, Harlin J, Lindström G (1992) Spillway design floods in Sweden: I. New Guidelines Hydrol Sci J 37:505–519

Bizuneh BB, Moges MA, Sinshaw BG, Kerebih MS (2021) SWAT and HBV models' response to streamflow estimation in the upper Blue Nile Basin. Ethiopia Water-Energy Nexus 4:41–53

Carvajal PE, Anandarajah G, Mulugetta Y, Dessens O (2017) Assessing uncertainty of climate change impacts on long-term hydropower generation using the CMIP5 ensemble—the case of Ecuador. Climatic Change 144:611–624

Carvajal PE, Li FG, Soria R, Cronin J, Anandarajah G, Mulugetta Y (2019) Large hydropower, decarbonisation and climate change uncertainty: modelling power sector pathways for Ecuador. Energy Strat Rev 23:86–99

Casale F, Bombelli G, Monti R, Bocchiola D (2020) Hydropower potential in the Kabul River under climate change scenarios in the XXI century. Theoret Appl Climatol 139:1415–1434

Felfelani F, Movahed AJ, Zarghami M (2013) Simulating hedging rules for effective reservoir operation by using system dynamics: a case study of Dez Reservoir. Iran Lake and Reservoir Manag 29:126–140

Fowler HJ, Blenkinsop S, Tebaldi C (2007) Linking Climate Change Modelling to Impacts Studies: Recent Advances in Downscaling Techniques for Hydrological Modelling. Int J Climatol 27:1547–1578

Hargreaves GH, Samani ZA (1985) Reference crop evapotranspiration from temperature. Appl Eng Agric 1:96–99

IPCC (2007) Climate change 2007-impacts, adaptation and vulnerability: Working group II contribution to the fourth assessment report of the IPCC, vol 4. Cambridge University Press

IPCC (2013) Climate Change 2013: The physical science basis. In: Stocker TF, Qin D, Plattner G-K, Tignor M, Allen SK, Boschung J, Nauels A, Xia Y, Bex V, Midgley PM (eds) Contribution of working group I to the fifth assessment report of the intergovernmental panel on climate Change. Cambridge University Press, Cambridge, United Kingdom and New York, NY, USA, pp 1535

IWPCO (2009) Studies of the second phase of Khersan3 reservoir dam and electric power plant project. Technical report on water resource planning, energy analysis, and hydroelectric power (Available in Persian). Iran Water and Power Resources Development Company Press, Tehran, Iran, pp 127

Kamali M, Ponnambalam K, Soulis E (2007) Computationally efficient calibration of WATCLASS Hydrologic models using surrogate optimization. Hydrol Earth Syst Sci Discussions 4:2307–2321

Khazaei MR (2021) A robust method to develop future rainfall IDF curves under climate change condition in two major basins of Iran. Theoret Appl Climatol 144:179–190

Khazaei MR, Zahabiyoun B, Saghafian B (2012) Assessment of climate change impact on floods using weather generator and continuous rainfall-runoff model. Int J Climatol 32:1997–2006

Khazaei MR, Zahabiyoun B, Saghafian B, Ahmadi S (2014) Development of an automatic calibration tool using genetic algorithm for the ARNO conceptual rainfall-runoff model. Arab J Sci Eng 39:2535–2549

Khazaei MR, Zahabiyoun B, Hasirchian M (2020a) Comparison of IWG and SDSM weather generators for climate change impact assessment. Theoret Appl Climatol 140:859–870. https://doi.org/10.1007/s00704-020-03119-1

Khazaei MR, Zahabiyoun B, Hasirchian M (2020b) A new method for improving the performance of weather generators in reproducing low-frequency variability and in downscaling. Int J Climatol 40:5154–5169. https://doi.org/10.1002/joc.6511

Kumar A, Schei T, Ahenkorah A, Caceres Rodriguez R, Devernay J -M, Freitas M, Hall D, Killingtveit A, Liu A (2011) Hydropower. In: Edenhofer O, Pichs-Madruga R, Sokona Y, Seyboth K, Matschoss P, Kadner S, Zwickel T, Eickemeier P, Hansen G, Schlomer S, von Stechow C (eds) IPCC special report on renewable energy sources and climate change mitigation. Cambridge University Press, Cambridge, United Kingdom and New York, NY, USA

Liang H, Zhang D, Wang W, Yu S, Wang H (2023) Quantifying future water and energy security in the source area of the western route of China's South-to-North water diversion project within the context of climatic and societal changes Journal of Hydrology. Reg Stud 47:101443

Loucks DP, Van Beek E (2017) Water resource systems planning and management: an introduction to methods, models, and applications. Springer

Lumbroso D, Woolhouse G, Jones L (2015) A review of the consideration of climate change in the planning of hydropower schemes in sub-Saharan Africa. Clim Change 133:621–633

Milly PC, Betancourt J, Falkenmark M, Hirsch RM, Kundzewicz ZW, Lettenmaier DP, Stouffer RJ (2008) Stationarity is dead: whither water management? Science 319:573–574

Mousavi RS, Ahmadizadeh M, Marofi S (2018) A multi-GCM assessment of the climate change impact on the hydrology and hydropower potential of a semi-arid basin (A case study of the Dez Dam Basin, Iran). Water 10:1458

Mukheibir P (2013) Potential consequences of projected climate change impacts on hydroelectricity generation. Clim Change 121:67–78

Natalia P, Silvia F, Silvina S, Miguel P (2020) Climate change in northern Patagonia: critical decrease in water resources. Theor Appl Climatol 140:1–16

Neelakantan T, Sasireka K (2013) Hydropower reservoir operation using standard operating and standard hedging policies International Journal of. Eng Technol 5:1191–1196

Nonki RM, Lenouo A, Lennard CJ, Tchawoua C (2019) Assessing climate change impacts on water resources in the Benue River Basin. Northern Cameroon Environ Earth Sciences 78:1–18

Nonki RM, Lenouo A, Tshimanga RM, Donfack FC, Tchawoua C (2021) Performance assessment and uncertainty prediction of a daily time-step HBV-Light rainfall-runoff model for the Upper Benue River Basin. Northern Cameroon J Hydrol: Regional Studies 36:100849

Oyerinde GT, Wisser D, Hountondji FC, Odofin AJ, Lawin AE, Afouda A, Diekkrüger B (2016) Quantifying uncertainties in modeling climate change impacts on hydropower production. Climate 4:34

Qin P, Xu H, Liu M, Du L, Xiao C, Liu L, Tarroja B (2020) Climate change impacts on Three Gorges Reservoir impoundment and hydropower generation. J Hydrol 580:123922

Radmanesh F, Esmaeili-Gisavandani H, Lotfirad M (2022) Climate change impacts on the shrinkage of Lake Urmia Journal of Water and Climate. Change 13:2255–2277

Seibert J (2000) Multi-criteria calibration of a conceptual runoff model using a genetic algorithm. Hydrol Earth Syst Sci 4:215–224

Seibert J, Vis MJ (2012) Teaching hydrological modeling with a user-friendly catchment-runoff-model software package. Hydrol Earth Syst Sci 16:3315–3325

Semenov MA, Stratonovitch P (2010) Use of multi-model ensembles from global climate models for assessment of climate change impacts. Clim Res 41:1–14

Semenov MA, Brooks RJ, Barrow EM, Richardson CW (1998) Comparison of the wgen and lars-wg stochastic weather generators for diverse climates. Clim Res 10:95–107

Shrestha A, Shrestha S, Tingsanchali T, Budhathoki A, Ninsawat S (2021) Adapting hydropower production to climate change: a case study of Kulekhani Hydropower Project in Nepal. J Clean Prod 279:123483

Solaymani S (2021) A Review on Energy and Renewable Energy Policies in Iran. Sustainability 13:7328

Stucchi L, Bombelli GM, Bianchi A, Bocchiola D (2019) Hydropower from the Alpine cryosphere in the era of climate change: the case of the Sabbione Storage Plant in Italy. Water 11:1599

Stucchi L, Bocchiola D, Simoni C, Ambrosini SR, Bianchi A, Rosso R (2023) Future hydropower production under the framework of NextGenerationEU: the case of Santa Giustina reservoir in Italian Alps. Renewable Energy 215:118980

Tayebiyan A, Ali TAM, Ghazali AH, Malek M (2016) Optimization of exclusive release policies for hydropower reservoir operation by using genetic algorithm. Water Resour Manage 30:1203–1216

ulShafiq M, Ramzan S, Ahmed P, Mahmood R, Dimri A (2019) Assessment of present and future climate change over Kashmir Himalayas India. Theor Appl Climatol 137:3183–3195

Zamani Y, HashemiMonfared SA, AzhdariMoghaddam M, Hamidianpour M (2020) A comparison of CMIP6 and CMIP5 projections for precipitation to observational data: the case of Northeastern Iran. Theor Appl Climatol 142:1613–1623

Zhang G, Savenije H (2005) Rainfall-runoff modelling in a catchment with a complex groundwater flow system: application of the Representative Elementary Watershed (REW) approach. Hydrol Earth Syst Sci Discussions 9:243–261

Zhao Y, Xu K, Dong N, Wang H (2022) Projection of climate change impacts on hydropower in the source region of the Yangtze River based on CMIP6. J Hydrol 606:127453

Zhao X, Huang G, Li Y, Lu C (2023) Responses of hydroelectricity generation to streamflow drought under climate change. Renew Sustain Energy Rev 174:113141

Zhou Q, Hanasaki N, Fujimori S, Masaki Y, Hijioka Y (2018) Economic consequences of global climate change and mitigation on future hydropower generation. Clim Change 147:77–90